PHYSICAL REVIEW B **79**, 134418 (2009)

Stripe patterns in underdoped cuprates compatible with magnetic neutron scattering data

E. P. Stoll and P. F. Meier
Physics Institute, University of Zurich, CH-8057 Zurich, Switzerland
(Received 25 June 2008; revised manuscript received 25 March 2009; published 14 April 2009)

In the insulating phase the cuprates exhibit long-ranged antiferromagnetic order which, however, breaks down when they are doped to become metallic. Neutron scattering data show that upon doping the width w of the magnetic structure factors $S(\vec{q})$ becomes broader and that their centers shift away from the antiferromagnetic wave vector by an amount δ which grows with increasing doping concentration. The spatial two-point spin correlation can directly be determined from $S(\vec{q})$. Using the information available from the position and width of $S(\vec{q})$ and assuming random spin phase distributions, we calculated the spin arrangement $\vec{s}_m$ in direct space. $\vec{s}_m$ exhibits patterns of vertical and horizontal stripes of finite length such as a two-dimensional nematic fluid. The finite length depends on the width w whereas the distance between two neighboring stripes is proportional to δ. Furthermore, the differences between experimental results obtained by neutron scattering and by nuclear magnetic resonance are discussed.

DOI: 10.1103/PhysRevB.79.134418 PACS number(s): 74.25.Ha, 74.62.Dh, 75.25.+z, 75.30.Gw

I. INTRODUCTION

The parent compounds of perovskite cuprate superconductors are insulators and exhibit quasi two-dimensional antiferromagnetic (AFM) order in the CuO_2 planes with weak couplings to adjacent planes. The spins reside mainly on the copper ions. Only by doping with holes, e.g., substituting La^{3+} by Sr^{2+} in $La_{2-x}Sr_xCuO_4$ (LASCO) or adding oxygen in $YBa_2Cu_3O_{6+y}$ (YBCO), electric conduction is established. For very small concentrations of dopant atoms these systems remain antiferromagnetic insulators with the spin arrangement in the planes described by

$$\vec{s}_m = \vec{s}_0(-1)^{m_x+m_y}, \tag{1}$$

where m_x and m_y are the x and y components of the copper site m. Upon further doping the antiferromagnetic order parameter vanishes and spin-glass-like states occur. This means that the antiferromagnetic long-range spin correlation breaks down and only a short-range correlation with changing arrangements of spins lying in different domains exists,

$$\vec{s}_m = \vec{s}_0(-1)^{m_x+m_y}p_m. \tag{2}$$

p_m can take the values 1 or −1, depending on the particular domain. Coppers between two domains (in domain walls) can have no magnetic moment and are denoted by $p_m=0$. Increasing doping transforms the system from an insulator into an electric conductor which at temperatures below the transition temperature T_c exhibits superconductivity. T_c becomes larger with increasing doping, reaches a maximum, and then declines for even larger doping.

The picture of the spin arrangement is thus very simple in the undoped parent compounds. For doped systems, however, it becomes rather complicated and it leads to controversies by comparing[1] the results from nuclear quadrupole resonance (NQR) and nuclear magnetic resonance (NMR) experiments[2] with those from magnetic neutron scattering.[3–6]

Of particular interest is the formation of stripes that occurs in a certain range of doping concentration. In the simplest version of a stripe arrangement doped holes are confined by antiferromagnetic domain wall lines. Theoretically, stripes were predicted by Zaanen and Gunnarsson[7] who treated a three-band Hubbard model in the Hartree-Fock approximation. Later studies which went beyond the simple mean-field treatment of Ref. 7 showed that the phenomenon of stripes is rather robust. Experimentally, stripes were first found by neutron scattering in nickelates.[8] Later, stripelike features were also observed in cuprates (For a review, see Ref. 1).

For the undoped insulating materials, the magnetic structure factors $S(\vec{q})$ are peaked at the antiferromagnetic wave vector $\vec{Q}=(\pi/a,\pi/a)$, where a is the CuO_2 plane lattice constant. In the doped materials, however, the measured peaks are located at $\vec{Q}_{c,j}$, which are shifted from $\vec{Q}$ by $(0,\pm\delta/a)$, $(\pm\delta/a,0)$, and $j=1,\ldots,4$. The shifts δ increase with increasing doping concentrations, and the half-widths of the peaks grow.

From the measured $S(\vec{q})$ the two-point spin correlation function in the direct space can be determined. Due to the lack of information on the phases of the spin values observed in neutron scattering, however, a reconstruction of the spin arrangement in direct space is not possible.

In the present work we assume that the phases are uncorrelated and determine spin arrangements in direct space. The structure factors calculated from these theoretical direct space spin distributions are in good agreement with the measured $S(\vec{q})$. In Sec. II the impact of holes on the spin and charge distribution of the CuO_2 plane is summarized. In Sec. III spin distributions and Fourier spectra are discussed. Sec. IV contains the summary and conclusions.

II. IMPACT OF HOLES

Because the copper oxides have to be doped to become electric conductors or superconductors, metallic ions with different valences (e.g., Sr or Ba instead of La) have to be substituted or further oxygen atoms have to be added. In the commonly adopted ionic picture, the copper atoms are in the $3d^9$ state, thus carrying a single intrinsic hole with spin 1/2. In the antiferromagnetically ordered system the four Cu

neighbors then deliver an energy gain of four times the exchange energy.

Additional holes (or electrons) change the spin arrangements. Zhang and Rice[9] put forward a model where one extrinsic hole occupies the diamond-shaped tetragon between four oxygen atoms in the CuO_2 plane and alters simultaneously the total copper and oxygen charge and spin. The particular copper spin at site m is either compensated or shielded into the so-called Zhang-Rice singlet[9] and acts like a spin with value zero, and thus p_j in Eq. (2) becomes zero. The corresponding loss in antiferromagnetic exchange energy may be compensated by gains in kinetic energy or by gains due to the formation of stripes.

The basic reasons for the formation of stripes in the frame of the Hubbard or t-J model are given in Ref. 1 (see, e.g., Fig. 2.6). An array of holes is energetically disadvantageous due to the Coulomb repulsion. Holes on a domain wall, however, can move unimpeded by the spin system. In contradiction to one-dimensional stripe structures[10] the two-dimensional stripe arrangements are in accordance with recent neutron scattering measurements[6] on nearly fully untwinned $YBa_2Cu_3O_{6+x}$ crystals.

III. SPIN DISTRIBUTIONS AND FOURIER SPECTRA

The magnetic scattering function measured with neutrons can be written as[11]

$$S(\vec{q},\omega) = \sum_{\alpha,\beta} [\delta_{\alpha,\beta} - q_\alpha q_\beta/q^2] S_{\alpha\beta}(q,\omega), \tag{3}$$

where

$$S_{\alpha\beta}(q,\omega) = \frac{1}{2\pi}\int dt e^{-i\omega t} \sum_{\vec{m}} e^{i\vec{q}\vec{r}_{\vec{m}}} \langle s_0^\alpha(0) s_{\vec{m}}^\beta(t)\rangle. \tag{4}$$

Here $s_{\vec{m}}^\beta(t)$ denotes the β component of the atomic spin at lattice site $\vec{r}_{\vec{m}}$ at time t. In the following we focus on the equal time two-point spin correlation function:

$$g_{\vec{m}}^{\alpha\beta} = \langle s_0^\alpha s_{\vec{m}}^\beta\rangle \propto \int d^3q e^{i\vec{q}\vec{r}_{\vec{m}}} S_{\alpha\beta}(\vec{q}), \tag{5}$$

where the angle brackets denote an average over configurations. In experiments, different scattering geometries and mostly nonpolarized neutrons are used. For inelastic scattering $S(\vec{q},\omega)$ is proportional to the imaginary part of the spin susceptibility $\chi''(\vec{q},\omega)$. Therefore, we consider the main component of the diagonal part of the tensor quantity $g_{\vec{m}}^{\alpha\beta}$ which we denote simply by $g_{\vec{m}}$,

$$g_{\vec{m}} = \langle s_0^z s_{\vec{m}}^z\rangle \propto \int d^3q e^{i\vec{q}\vec{r}_{\vec{m}}} S(\vec{q}). \tag{6}$$

Note, however, that this z component does not refer to the crystallographic z direction but rather lies in the xy plane depending on the particular experimental situation.

In first approximation, the structure factor[3–5] measured for $La_{2-x}Sr_xCuO_4$ or for $YBa_2Cu_3O_7$ can be described by the sum of four delta functions[12]

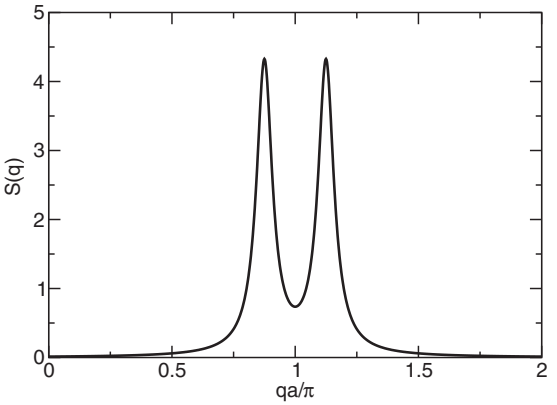

FIG. 1. Fourier spectrum of the spin distribution in one dimension. $|Q_{c,j} - \pi/a| = 1/8 \times \pi/a$, $\xi_G = 8a$, $\xi_L = 2a$, and $\xi = 8.246a$.

$$S(\vec{q}) \propto \sum_j \delta(\vec{q} - \vec{Q}_{c,j}), \tag{7}$$

where $\vec{Q}_{c,j}$ denote the centers of the four peaks ($j = 1,\ldots,4$). These delta functions are broadened due to limited instrumental resolution[13] as well as due to physical properties of the investigated material. In the following it is assumed that the instrumental resolution has already been taken into account and that the broadening is related only to deviations of the spin distributions from perfect alignment.

The broadening is described by a Gaussian distribution,

$$S(\vec{q}) \propto \sum_j \exp\{-[\xi_G(\vec{q} - \vec{Q}_{c,j})]^2\}. \tag{8}$$

It is well known that static structure factors can well be modeled by Gaussian distributions. On the other hand for dynamic structure factors Lorentzian-shaped distributions are often more appropriate. Since the neutron scattering data[3–5] have been obtained from inelastic measurements for low energy transfers ($\hbar\omega$ is in the order of a few meV), we have applied for the further investigations a combination of Gaussian and Lorentzian distributions as follows:

$$S(\vec{q}) \propto \sum_j \frac{\exp\{-[\xi_G(\vec{q} - \vec{Q}_{c,j})]^2\}}{1 + [\xi_L(\vec{q} - \vec{Q}_{c,j})]^2}. \tag{9}$$

Defining $\xi \propto 1/w$ by

$$\xi^2 = \xi_G^2 + \xi_L^2, \tag{10}$$

with w the half-widths of the peaks, the broadening is $e^{-\xi^2(\vec{q}-\vec{Q}_{c,j})^2}$ for $\xi^2(\vec{q} - \vec{Q}_{c,j})^2 \ll 1$.

We note that this combination of Gaussian and Lorentzian distributions is not essential for the discussion of the physical nature of the spin arrangements. It has, however, some technical advantages as will be seen later.

A. One-dimensional case

In this subsection, only one-dimensional distributions in q are investigated. As an example, $S(q)$ is shown in Fig. 1 with

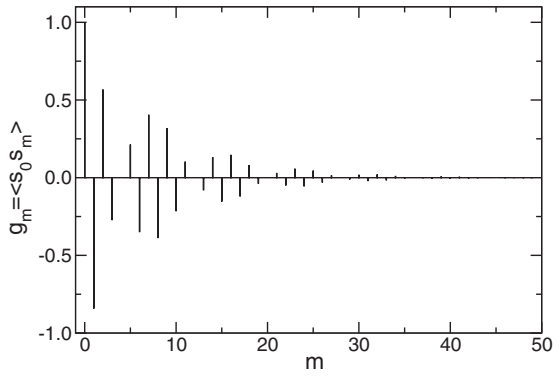

FIG. 2. Two-point correlation of the spin distribution in one dimension. The black lines denote g_m obtained by Fourier transformation [Eq. (6)] of the spectrum $S(q)$ shown in Fig. 1. $|Q_{c,j}-\pi/a|=1/8\times\pi/a$, $\xi_G=8a$, $\xi_L=2a$, and $\xi=8.246a$.

two peaks located at $|Q_{c,j}-\pi/a|=1/8\times\pi/a$ with $\xi_G=8a$, $\xi_L=2a$, and $\xi=8.246a$. This corresponds to a hole doping concentration of 1/8. Note that within the model a change in hole concentration will change these parameter values. The associated two-point correlation is displayed in Fig. 2.

A reconstruction of the direct space spin distribution s_m from $S(q)$ is not possible since the structure factor is proportional to the absolute square of $s(q)$,

$$S(q) \propto |s(q)|^2, \tag{11}$$

and no information on the phases $\varphi(q)$,

$$s(q) = |s(q)|\exp[i\varphi(q)], \tag{12}$$

is available from the experiments. We assume that the phases $\varphi(q)$ and $\varphi(q')$ are uncorrelated for $q \neq q'$. According to the spin-wave approximation, the eigenfrequencies of $S(q)$ are different from that of $S(q')$. Thus $s(q)$ is proportional to

$$s(q) \propto \sqrt{S(q)}\exp[i\varphi(q)], \tag{13}$$

and by Fourier back transformation one obtains

$$s_m \propto \int dq\, \exp(-iqr_m)s(q). \tag{14}$$

Using Eq. (14) the spin distributions are reconstructed by assuming that all spins are either +1 or −1 as follows:

$$\sigma_m = \mathrm{sign}[s_m]. \tag{15}$$

The spin distribution, which corresponds to the spectrum shown in Fig. 1 and determined by assuming uncorrelated phases, is displayed in Fig. 3(a). It is seen that most nearest neighbors are antiferromagnetically aligned but some (marked by gray areas) are ferromagnetically aligned. These energetically unfavorable arrangements at sites m and $m+1$ are now replaced by assigning a spin 0 to the site m. The resulting modified spin distribution is denoted by $\tilde{\sigma}_m$ and is shown in Fig. 3(b).

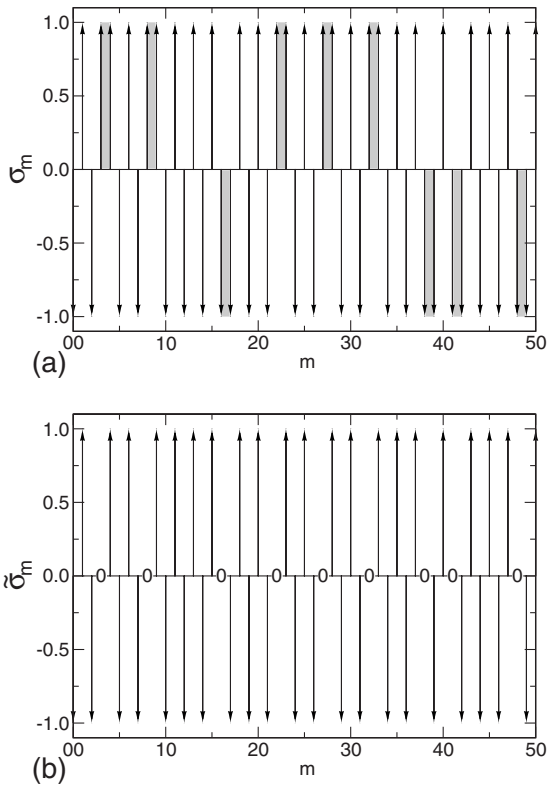

FIG. 3. Spin arrangement in one dimension. The gray areas in (a) show those neighboring spins which point in the same direction leading to higher energy state. In (b) the modified spin polarization distribution is shown where some copper sites have spin zero (marked by 0).

The motivation for modification of the distribution σ_m into $\tilde{\sigma}_m$ follows the arguments given by Brom and Zaanen.[1] The singlet states introduced by the extrinsic holes no longer interact magnetically with the neighbor copper spins plotted in Fig. 2.6 of Ref. 1. Therefore, a spin to the left part of the gray areas in Fig. 3(a) is replaced by a spin with value of 0. Then, as shown in Fig. 3(b), the neighboring spins of the hole are now antiparallel arranged, leading to lower energies.

From this modified spin distribution a modified two-point spin correlation,

$$\tilde{g}_m = \langle \tilde{\sigma}_0 \tilde{\sigma}_m \rangle, \tag{16}$$

is calculated and shown in Fig. 4. The corresponding Fourier spectrum,

$$\tilde{\Sigma}(q) \propto \int dr\, \exp(iqr_m)\tilde{g}_m, \tag{17}$$

is shown in Fig. 5.

The average distance between two holes accounts here for eight lattice constants in accordance with the locations of the peak maxima at $Q_{c,j}$ and $|Q_{c,j}-\pi/a|=1/8\times\pi/a$. Assumed fluctuations of these distances are the reason for the finite widths of the peaks in $S(q)$.

The spectrum $\tilde{\Sigma}(q)$ shown in Fig. 5 which has been evaluated from the modified spin distribution [plotted in Fig. 3(b)] can now be compared with the original Fourier spectrum

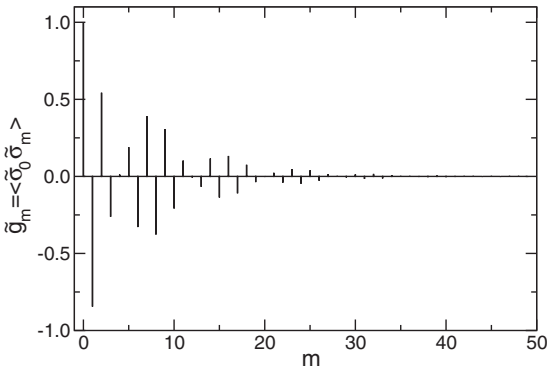

FIG. 4. Correlation of the modified spin distribution in one dimension. The black lines denote $\tilde{g}_m$ [Eq. (16)] with $\xi=8.246a$ and $|Q_{c,j}-\pi/a|=1/8\times\pi/a$.

$S(q)$ that is depicted in Fig. 1. The former spectrum shows at $qa/\pi=0.625$ and $qa/\pi=1.375$ small additional peaks. These peaks correspond to higher harmonics because it has been assumed that all spins of $\tilde{s}_m$ can only have the values +1, −1, or 0. The phases of the excitations at $qa/\pi=0.625$ and 1.375 are therefore correlated with those at $qa/\pi=0.875$ and 1.125. Applying a Gaussian with $\xi_L=2$ [Eq. (9)] the artifacts due to the absence of the correlation by purely random phases can almost be fully suppressed. Both spectra, $\tilde{\Sigma}(q)$ (Fig. 5) with $\xi_G=8$ and $\xi_L=2$ and $S(q)$ (Fig. 1) with $\xi_G=8.246$ and $\xi_L=0$ differ only by a very small amount in the height of the main peak maxima and the occurrence of the small higher harmonics at $qa/\pi=0.625$ and 1.375 in $\tilde{S}(q)$.

Therefore, also the two-point correlations $g_m=\langle s_0 s_m\rangle$ (see Fig. 2) do not differ very much from $\tilde{g}_m=\langle\tilde{\sigma}_0\tilde{\sigma}_m\rangle$ in Fig. 4. Both correlation functions are nearly identical, particularly the nearest-neighbor ($m=1$) correlation. Both g_4 and g_{12} vanish. This corresponds to the occurrence of the peak maxima at $Q_{c,j}$ and $|Q_{c,j}-\pi/a|=1/8\times\pi/a$. The finite peak widths in Fig. 5 characterized by finite ξ_G and ξ_L appear also in an exponential or Gaussian fast decrease in g_m and $\tilde{g}_m$ for larger m and can be traced back to fluctuations of the distances between succeeding holes in Fig. 3(b).

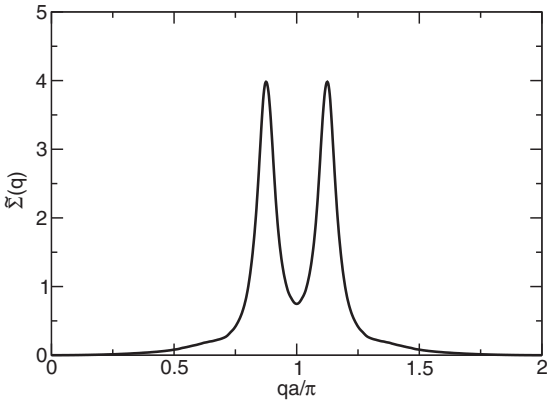

FIG. 5. Fourier spectrum of the spin distribution $\tilde{\Sigma}(q)$ in one dimension according Eq. (17) with $\xi=8.246a$ and $|Q_{c,j}-\pi/a|=1/8\times\pi/a$.

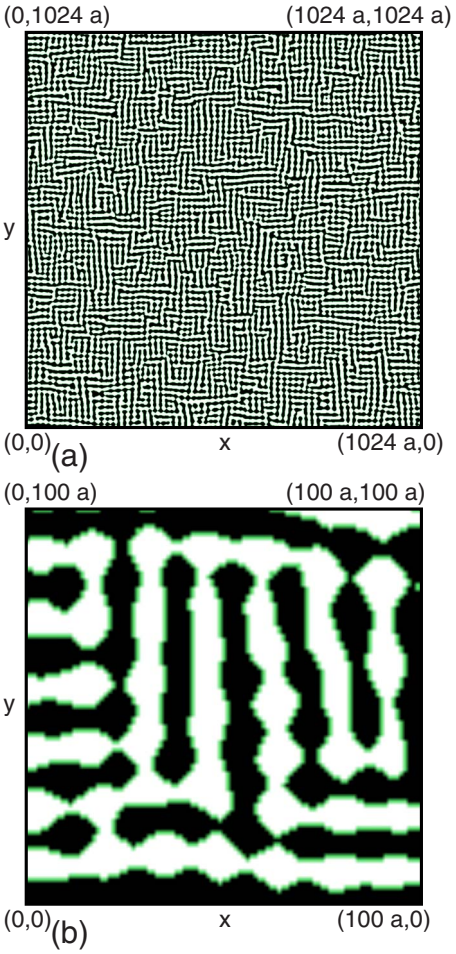

FIG. 6. (Color online) Two-dimensional spin arrangement calculated in direct space. (a) Large system. (b) Zoom of a part of (a). White regions denote $\tilde{\sigma}_{m_x,m_y}$ with $p=+1$ of Eq. (2) and black regions with $p=-1$. They are separated by gray (green) borders with $p=0$. $|\vec{Q}_{c,j}-(\pi/a,\pi/a)|=1/8\times\pi/a$, $\xi_G=15a$, and $\xi_L=0a$.

B. Two-dimensional case

In neutron scattering data[4,5] with all scattering vectors lying in the CuO_2 plane, the maxima of $S(\vec{q})$ are located at $\vec{Q}_{c,j}=(Q_c,0)$, $(-Q_c,0)$, $(0,Q_c)$, and $(0,-Q_c)$. Using a similar formalism as in one dimension the quantities $s(\vec{q})$, s_m, σ_m, and $\tilde{\sigma}_m$ can be determined by using Eqs. (13)–(15) and the relations given by Eqs. (16) and (17). In Fig. 6 the spins are arrayed in direct space with $p=+1$ of Eq. (2) (white clusters) and with $p=-1$ (black clusters). These clusters are separated by gray (green) borders where $p=0$. White and black regions form finite horizontal and vertical stripelike patches. Because $|\vec{Q}_{c,j}-(\pi/a,\pi/a)|=1/8\times\pi/a$ the average distance between two patches with the same color is 16 a. From these spin distributions also $\tilde{\Sigma}(\vec{q})$ and $\tilde{g}_m=\langle\tilde{\sigma}_0\tilde{\sigma}_m\rangle$ are calculated (see Fig. 8).

Our patch distribution shown in Fig. 6 answers the question asked in Ref. 1 of how the regions that have either horizontal or vertical arranged stripes can be separated. The energy is lower for very long stripes. On the other hand, the entropy term in the free energy favors small stripe length.

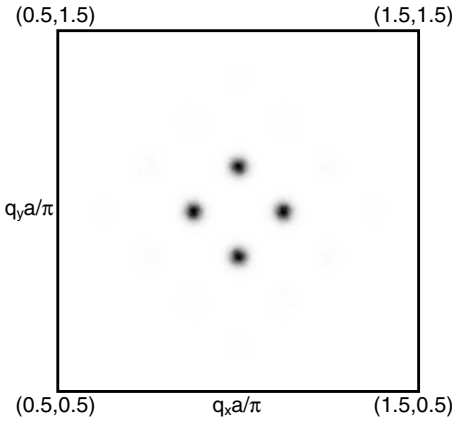

FIG. 7. Fourier spectrum $\tilde{\Sigma}(\vec{q})$ of a spin distribution $\tilde{\sigma}_{m_x,m_y}$ in two dimensions. The darkest part of the peaks is $1/8\times\pi/a$ apart from the antiferromagnetic point $(\pi/a,\pi/a)$. $|\vec{Q}_{c,j}-(\pi/a,\pi/a)|=1/8\times\pi/a$, $\xi_G=15a$, and $\xi_L=0a$.

This balancing is mapped in the neutron scattering data by the width of the peaks in the $\vec{q}$ space.

From the two-dimensional spin arrangement displayed in Fig. 6 the structure factor $\tilde{\Sigma}(\vec{q})$ is recalculated (see Fig. 7). This $\tilde{\Sigma}(\vec{q})$ can now be compared with the peaks measured by magnetic neutron scattering.[4,5] The agreement is excellent. The spatial arrangement of the calculated peaks in q space corresponds to the two-point correlation function $\tilde{g}_m$ in direct space shown in Fig. 8 which exhibits large squares turned by 45°.

As shown in the one-dimensional case in Fig. 4, the two-point correlation reaches its maximum for $x=0$ and $y=0$. Then for $x=8a$ and $y=0$ a gray color appears denoting no correlation. This correlationless band is continued through the hole picture in $\pm 45°$ directions and is continued for $x=24a$ and $y=0$. Furthermore, the correlation maxima become weaker with increasing distance from the coordinate origin. As in one dimension this is due to the distance fluctuations

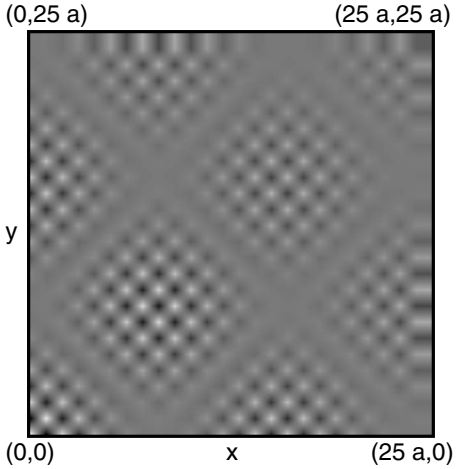

FIG. 8. Spin-spin correlation in two dimensions. Positive correlations are white or bright, and negative correlations are black or dark. Grey squares denote correlations close to zero. $|\vec{Q}_{c,j}-(\pi/a,\pi/a)|=1/8\times\pi/a$, $\xi_G=15a$, and $\xi_L=0a$.

between black-and-white-dot-like spots in Fig. 6(b) and corresponds to the finite peaks widths in Fig. 7.

At this point it is appropriate to discuss the difference of experimental results obtained by neutron scattering and by NMR or muon spin rotation spectroscopy (μSR). NMR and μSR are local probes and sensitive to fluctuations with characteristic frequencies in the order of GHz or lower. Neutrons, on the other hand, are a global probe, and the data[3–5] discussed above have been obtained from dynamic measurements in the scale of THz.

We first comment on the local versus global probe aspects. In view of Fig. 6 the neutrons see the periodic arrays of the stripes. Thus the shifts of the spin-fluctuation peaks away from the AFM wave vector reflect rather the appearance of discommensuration[14] than incommensuration. Within a particular domain where the local probes measure, the short-range AFM correlation is still present. For an oxygen nucleus, in particular, the spin-lattice relaxation rate depends on the magnetic moments located on its two nearest-neighbor copper ions which are antiferromagnetically correlated.

As this concerns the dynamics, we note that the patterns depicted in Fig. 6 correspond to a snapshot taken on the time scale of 10^{-12} s. For longer times, it is expected that the stripelike patterns change and meander in the CuO_2 plane. For NMR and μSR experiments most of the dynamics of these patches are averaged out. The nearest-neighbor AFM correlation survives the longest but most likely with a reduced absolute value. The correlations between a spin and its second and third neighbors, which affect the copper spin-lattice relaxation, decay earlier. Generally, the spatial AFM correlation length observed with NMR and μSR is likely appreciably shorter than that determined from neutron scattering.

It should be noted that other experiments also show space-modulated structures, in particular, resonant x-ray scattering and scanning tunneling spectroscopy.[15–17] These measurements, however, are sensitive to the surface of the sample. The influence of the time scale, which has been mentioned above, is also important for interpretation of these measurements but out of the scope of the present investigation.

IV. SUMMARY AND CONCLUSIONS

The spin-fluctuation spectrum in $La_{2-x}Sr_xCuO_4$ measured with magnetic neutron diffraction shows at low temperatures four peaks centered at $\vec{Q}_{c,j}$. The distance of each $\vec{Q}_{c,j}$ from the antiferromagnetic wave vector increases with Sr doping.[18] This implies the occurrence of antiferromagnetism modified by incommensurable spin arrangements. We have shown how such spectra can be simulated by using the values of $\vec{Q}_{c,j}$ and the width of the measured peaks as parameters. Furthermore, uncorrelated random phases have been applied to reconstruct the complex spin distribution $s(\vec{q})$ in the $\vec{q}$ space. In the direct space, however, the spin distribution $\tilde{s}_m$ is modified since the introduction of holes leads to the formation of Zhang-Rice[9] singlets which locally destroy the AFM order. The resulting spin arrangement $\tilde{s}_m$ yields

regions containing spins ordered with $p=+1$ of Eq. (2) and with $p=-1$ which are separated by horizontal and vertical stripes with $p=0$ as they are predicted by application of the t-J model.[1] The reduction in the exchange energy given by the parameter J can overcompensate the energy increase by the Coulomb repulsion of the holes in the chaines.[1] Our two-dimensional stripe arrangements are supported by recent neutron scattering data.[6] Finally, the two-point correlation functions $\tilde{g}_m$ and the spin-fluctuation spectrum $\tilde{\Sigma}(\vec{q})$ have been recalculated und discussed.

ACKNOWLEDGMENTS

We acknowledge the help of C. P. Slichter and thank M. Mali for numerous enlightening discussions.

[1] H. B. Brom and J. Zaanen, in *Handbook of Magnetic Materials*, edited by K. H. J. Buschow (Elsevier, Amsterdam, 2003), Vol. 15, pp. 379–496.
[2] Y. Zha, V. Barzykin, and D. Pines, Phys. Rev. B **54**, 7561 (1996).
[3] T. R. Thurston, R. J. Birgeneau, M. A. Kastner, N. W. Preyer, G. Shirane, Y. Fujii, K. Yamada, Y. Endoh, K. Kakurai, M. Matsuda, Y. Hidaka, and T. Murakami, Phys. Rev. B **40**, 4585 (1989).
[4] S. W. Cheong, G. Aeppli, T. E. Mason, H. Mook, S. M. Hayden, P. C. Canfield, Z. Fisk, K. N. Clausen, and J. L. Martinez, Phys. Rev. Lett. **67**, 1791 (1991).
[5] T. E. Mason, G. Aeppli, S. M. Hayden, A. P. Ramirez, and H. A. Mook, Phys. Rev. Lett. **71**, 919 (1993).
[6] V. Hinkov, S. Pailhès, P. Bourges, Y. Sidis, A. Ivanov, A. Kulakov, C. T. Lin, D. P. Chen, C. Bernhard, and B. Keimer, Nature (London) **430**, 650 (2004).
[7] J. Zaanen and O. Gunnarsson, Phys. Rev. B **40**, 7391 (1989).
[8] J. M. Tranquada, B. J. Sternlieb, J. D. Axe, Y. Nakamura, and S. Uchida, Nature (London) **375**, 561 (1995).
[9] F. C. Zhang and T. M. Rice, Phys. Rev. B **37**, 3759 (1988).
[10] H. A. Mook, P. Dai, F. Dogan, and R. D. Hunt, Nature (London) **404**, 729 (2000).
[11] G. L. Squires, *Introduction to the Theory of Thermal Neutron Scattering* (Dover, Mineola, NY, 1996).
[12] G. Aeppli, T. E. Mason, S. M. Hayden, H. A. Mook, and J. Kulda, Science **278**, 1432 (1997).
[13] H. A. Mook, P. Dai, S. M. Hayden, G. Aeppli, T. G. Perring, and F. Doğan, Nature (London) **395**, 580 (1998).
[14] C. P. Slichter (private communication).
[15] P. Abbamonte, A. Rusydi, S. Smadici, G. D. Gu, G. A. Sawabky, and D. F. Leng, Nat. Phys. **1**, 155 (2005).
[16] P. Abbamonte, Phys. Rev. B **74**, 195113 (2006).
[17] T. Valla, A. V. Fedorov, J. Lee, J. C. Davis, and G. D. Gu, Science **314**, 1914 (2006).
[18] K. Yamada, C. H. Lee, Y. Endoh, G. Shirane, R. J. Birgeneau, and M. A. Kastner, Physica C **282-287**, 85 (1997).